AD_____

MIPR NUMBER 96MM6721

TITLE: Contrast Enhancement of Mammograms By Optical Polarization of the Viewing Environment

PRINCIPAL INVESTIGATOR: David C. Spelic, Ph.D.

CONTRACTING ORGANIZATION: U.S. Food and Drug Administration
Laurel, Maryland 20708

REPORT DATE: October 1998

TYPE OF REPORT: Final

PREPARED FOR: Commander
U.S. Army Medical Research and Materiel Command
Fort Detrick, Frederick, Maryland 21702-5012

DISTRIBUTION STATEMENT: Approved for public release;
distribution unlimited

The views, opinions and/or findings contained in this report are those of the author(s) and should not be construed as an official Department of the Army position, policy or decision unless so designated by other documentation.

DTIC QUALITY INSPECTED 4

19990811 143

REPORT DOCUMENTATION PAGE

Form Approved
OMB No. 0704-0188

Public reporting burden for this collection of information is estimated to average 1 hour per response, including the time for reviewing instructions, searching existing data sources, gathering and maintaining the data needed, and completing and reviewing the collection of information. Send comments regarding this burden estimate or any other aspect of this collection of information, including suggestions for reducing this burden, to Washington Headquarters Services, Directorate for Information Operations and Reports, 1215 Jefferson Davis Highway, Suite 1204, Arlington, VA 22202-4302, and to the Office of Management and Budget, Paperwork Reduction Project (0704-0188), Washington, DC 20503.

1. AGENCY USE ONLY *(Leave blank)*	2. REPORT DATE	3. REPORT TYPE AND DATES COVERED
	October 1998	Final (15 May 96 - 30 Sep 98)

4. TITLE AND SUBTITLE
Contrast Enhancement of Mammograms By Optical Polarization of the Viewing Environment

5. FUNDING NUMBERS
96MM6721

6. AUTHOR(S)
David C. Spelic, Ph.D.

7. PERFORMING ORGANIZATION NAME(S) AND ADDRESS(ES)
U.S. Food and Drug Administration
Laurel, Maryland 20708

8. PERFORMING ORGANIZATION REPORT NUMBER

9. SPONSORING/MONITORING AGENCY NAME(S) AND ADDRESS(ES)
Commander
U.S. Army Medical Research and Materiel Command
Fort Detrick, Frederick, Maryland 21702-5012

10. SPONSORING/MONITORING AGENCY REPORT NUMBER

11. SUPPLEMENTARY NOTES

12a. DISTRIBUTION / AVAILABILITY STATEMENT
Approved for public release; distribution unlimited

12b. DISTRIBUTION CODE

13. ABSTRACT *(Maximum 200*

Purpose: To investigate the possibility that commercially available brands of mammography film may possess optical polarimetric properties and whether any observed polarimetric behavior displayed a dependence on film optical density.

Procedure: A polarimeter was constructed for performing optical experiments using the method of Azzam[2]. The Mueller matrix formalism was used to describe the results of the experiments. A prototype viewing device was constructed and evaluated by two radiologists.

Results: Polarimetric behavior was observed for all brands of film tested. Further investigation isolated the probable source of this behavior to the base of the film, rather than to the emulsion (which is responsible for the production of the image one sees). There is thus no observed evidence that mammography films display polarimetric behavior which is dependent on the optical density of the film. Results of the evaluation of the prototype suggest that the device may aid in the reading of films having low optical density (i.e. films that appear too light). However, the polarimetry results do not support the possibility that polarimetric behavior played a major role in this outcome.

14. SUBJECT TERMS	15. NUMBER OF PAGES
Breast Cancer	44
	16. PRICE CODE

17. SECURITY CLASSIFICATION OF REPORT	18. SECURITY CLASSIFICATION OF THIS PAGE	19. SECURITY CLASSIFICATION OF ABSTRACT	20. LIMITATION OF ABSTRACT
Unclassified	Unclassified	Unclassified	Unlimited

FOREWORD

Opinions, interpretations, conclusions and recommendations are those of the author and are not necessarily endorsed by the U.S. Army.

____ Where copyrighted material is quoted, permission has been obtained to use such material.

____ Where material from documents designated for limited distribution is quoted, permission has been obtained to use the material.

_X_ Citations of commercial organizations and trade names in this report do not constitute an official Department of Army endorsement or approval of the products or services of these organizations.

____ In conducting research using animals, the investigator(s) adhered to the "Guide for the Care and Use of Laboratory Animals," prepared by the Committee on Care and use of Laboratory Animals of the Institute of Laboratory Resources, national Research Council (NIH Publication No. 86-23, Revised 1985).

____ For the protection of human subjects, the investigator(s) adhered to policies of applicable Federal Law 45 CFR 46.

____ In conducting research utilizing recombinant DNA technology, the investigator(s) adhered to current guidelines promulgated by the National Institutes of Health.

____ In the conduct of research utilizing recombinant DNA, the investigator(s) adhered to the NIH Guidelines for Research Involving Recombinant DNA Molecules.

____ In the conduct of research involving hazardous organisms, the investigator(s) adhered to the CDC-NIH Guide for Biosafety in Microbiological and Biomedical Laboratories.

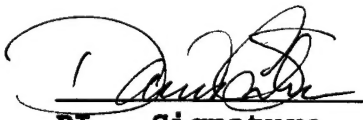

PI - Signature

11/18/98

Date

Table of Contents

Introduction

The goal of the project was to investigate the polarimetric properties of commercially available mammography x-ray films and determine whether any possessed optical properties that could be exploited in order to improve the visualization of relevant features on the x-ray film image. If such properties were found, a prototype viewing device would be designed in accordance with the optical properties so discovered. This final report to the U.S. Army reports on the findings and subsequent recommendations of this investigation.

Interest in the polarimetric properties of mammography films was motivated by the demand in mammography for a high degree of image contrast. Good contrast is necessary to visualize structures in the breast that promote only slight changes in exposure to the film. The technical aspects of film/screen mammography seem to be highly optimized at this point in time. These include the x-ray system, the films and screens used for image production, administered dose to the patient, and film processing. Yet the radiologist is still challenged with the evaluation of an image that contains a high degree of structural content against which minute features of interest lie. Digital systems are on the forefront and will provide a supply of tools unavailable to the film-screen modality. Cost will most likely drive many mammography facilities to continue using film-screen technology for some time, however.

This project examined the polarimetric properties of the majority of commercially available mammography film brands. Brands were selected based on the relative frequency of use by mammography facilities. This was determined from data collected as part of Mammography Quality Standards Act of 1992 (MQSA) inspections by the FDA. A possible outcome would be a device that would be used in conjunction with the standard viewbox as a means of improving on the perceived quality of the image without a substantial investment or re-engineering of the viewbox.

Terminology

Retarder : A device or material that introduces a relative phase shift between the rays of light transmitted parallel to, and normal to a specified axis (referred to as the optical axis) of the device or material. A quarter-wave plate, for example, introduces a phase shift of 90 degrees between those rays of light with a plane of vibration containing the optical axis, and those rays with a plane of vibration normal to the optical axis. Optical elements also used quite frequently are the half-wave plate and full-wave plate.

Dichroism: A property of some materials to selectively absorb light traveling in a specified plane of vibration within the material. Polaroid sun-glasses are an example of this behavior. A term given to optical components which display this behavior is *linear polarizer*.

Stokes Parameter: In the Stokes methodology, the state of polarization of a given ray of light is specified by a four-element vector, $\vec{S} = (S_1, S_2, S_3, S_4)$. The first element S_1 specifies the total intensity of the beam, while the remaining elements describe specific states of polarization:

S_1 : *linear horizontal or vertical polarization*

S_2: *linear polarization at* ± 45 *degrees*

S_3: *left – or right circular polarization.*

Mueller Matrix: A mathematical expression of the optical polarimetric properties of a given material. The Mueller matrix is a four-dimensional object which contains all the information necessary to describe how the optical material influences the polarimetric state of light incident on it. It operates on the vector representation of an incident ray of light (the Stokes vector) $\vec{S}$, to produce a transmitted (final) state of polarization, $\vec{S}' = [M]\vec{S}$.

Methodology

The expression of polarimetric properties is made using the Mueller matrix formalism, in which the polarimetric properties of a material are expressed as elements of a four-dimensional square matrix. In this formalism, various states of polarization are represented by a four-vector $\vec{S}$. Here the four-vector $\vec{S}$ has the form

$$\vec{S} = \begin{bmatrix} S_0 \\ S_1 \\ S_2 \\ S_3 \end{bmatrix},$$

and is referred to as a Stokes vector, as described briefly above. The four elements of the Stokes vector S_i are referred to as the Stokes parameters, so named after Sir George Gabriel Stokes(1819-1903), who discovered a means of describing polarimetric properties of light in terms of observables, namely light intensity. The Stokes parameters describe the nature and degree of polarization of the light so represented. Upon interacting with a medium, the polarization state of light will in general, be altered. The ability of materials to influence the polarimetric state of light is described by the Mueller matrix. The Mueller matrix $[M] = (m_{ij})$, $i,j = 1,2,3,4$ of a material consists of sixteen elements and is an analytical representation of the material's influence on various states of polarization. It operates on an incident polarization state $\vec{S}$ to produce a final polarization state $\vec{S}'$,

$$\vec{S}' = [M]\vec{S}.$$

In film/screen mammography film contrast is a quantity used to describe the ability of a film to record changes in exposure to the film as changes in optical density:

$$film\ contrast = \frac{d(Optical\ Density)}{d(Log\ Relative\ Exposure)} = \frac{dOD}{dLRE}\ .$$

As defined above, film contrast is essentially the first derivative, or slope of the Hurter-Driffield (H-D) curve of a radiographic film. It expresses the rate of change in optical density on the film with changes in exposure.

The human eye as well has a characteristic curve which describes the response of the eye to changes in levels of light[1]. Further, Tovée explains the apparent existence of an array of response curves for the human eye, each based on the level of background light against which features are viewed. This behavior, known as light adaptation, allows the human eye to respond to changes of light in a dark environment much the same as it would in a bright environment. Light adaptation requires a period of time, however, and thus invokes a challenge to the radiologist.

To alter the apparent contrast perceived by the eye when a radiograph is viewed, the relative amounts of light transmitted by adjacent regions on the radiograph must be manipulated. If two adjacent regions on the film possess differing optical polarimetric properties then it might be possible to influence the amounts of transmitted light with a suitable optical environment. Hence our efforts focused on determining to what extent radiographic films used for mammography possessed such optical polarimetric properties.

Progress since the first annual report

The first annual report submitted to the U.S. Army reported our efforts to establish a laboratory facility suitable for performing optical polarimetry. Some preliminary experimental data was also reported. Subsequent efforts focused toward refining the accuracy of the polarimeter and automating the data collection. The current system feeds the optical detector signal from the polarimeter into an amplifier, which is then read by a computer configured with an analog-to-digital converter board. Software controls both the micro-stepping motors which rotate optical elements and sampling of the A/D board for the optical detector signal.

The method of Azzam[2] was used to perform the polarimetric measurements. This method allows the determination of all sixteen elements which make up the Mueller matrix. A Quartz- Tungsten halogen lamp with a broad spectral emission peaking in the infrared was used as the light source for all measurements. To tailor the spectral distribution of the input source, a photopic filter was used to shape the source spectrum to the sensitivity of the human eye.

Software was written in Mathematica to model the generation of calibration (air) data for the polarimeter as well as model various polarimetric scenarios encountered/investigated during this study. Computer simulations were used to assess the experimental errors incurred due to alignment errors and imperfections in the optical components of the polarimeter.

Finally, a prototype viewing template was developed in accordance with experimental findings as well as criteria derived from the end-user(the radiologist). Among the criteria derived from the end-user, the device had to be:

1. Simple enough to use such that the radiologist would not find it over-burdensome to use on a routine basis.
2. Flexible enough to adapt to any film orientation (the optical axis of the film is not evident to the un-aided eye, nor does a radiologist typically concern him/herself with this when placing the film on the viewbox).
3. Account for some loss in intensity when polarizers are introduced into the viewing chain.

The prototype constructed with these criteria in mind was evaluated by two staff radiologists at the Center for Devices and Radiological Health. Readers were provided a sampling of actual clinical films covering a range of image quality levels, and also provided mammography films produced using phantoms containing test objects. Results of this aspect of the project will be discussed below.

The following experiments/analyses were carried out to investigate the optical polarimetric properties of mammography films:

1. P S P(ϑ) Polarimeter.
   Purpose: To observe the gross polarimetric behavior of samples of mammography film. The experiment employs two polarizers, with one polarizer, P(ϑ) rotated with respect to the stationary film sample S and second polarizer, P.

2. Mueller Matrix Polarimetry: P C(5ϑ) S C(ϑ) P experiments.
   Purpose: To determine and classify the polarimetric properties of film samples. Fourier analysis of resulting data allow construction of the Mueller matrix.

3. P S P(ϑ) polarimetry for the determination of the ratio β / α.
   Purpose: To verify the results of experiment 2, Mueller Matrix Polarimetry. Based on the results of experiment 2, further experiments were conducted using the set-up for experiment 1. This would verify the apparent form discovered for the Mueller matrix of mammography films.

4. Prototype Viewing Device
   Purpose: To construct a prototype viewing device and evaluate its effect on the apparent image quality of mammograms.

Experiment: P S P(ϑ) Polarimeter

Purpose: To observe gross optical polarimetric behavior of mammography films.

Procedure:

In this experiment a selected film sample S is positioned between two initially aligned polarizers, P1 and P2. Polarizer P2 is subsequently rotated through a series of angles. The transmitted light is measured with a photodetector. A diagram illustrating the set-up is given in Figure 1.

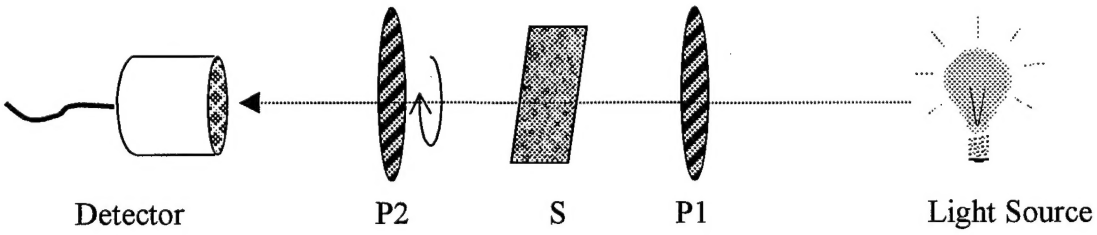

Figure 1. Illustration of experimental set-up for P S P polarimetry. P1 and P2 are linear (Glan-Thompson) polarizers and S is the film sample being studied.

Data is also acquired with the film sample rotated relative to the generator P1. This orients the optical axis of the sample S to different positions with respect to the orientation of light incident (produced by P1) on it. The light source used for this set of experiments was a quartz-tungsten halogen lamp having the spectral output shown in figure 2. Signals from the detector were amplified and then digitized for analysis by computer as diagrammed in figure 3.

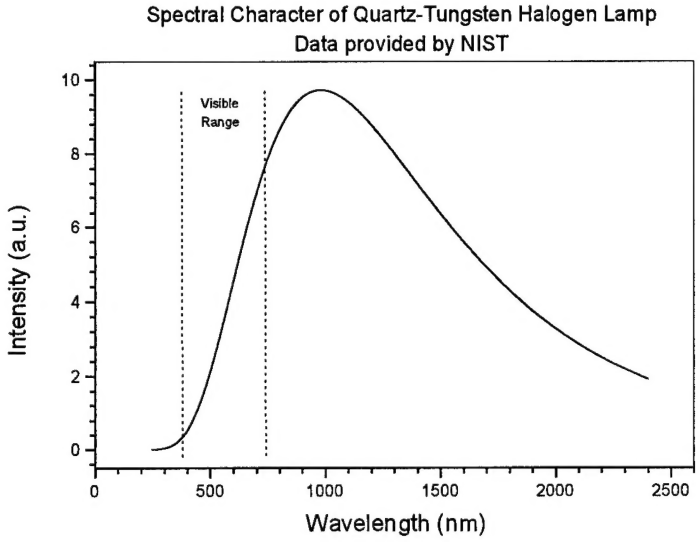

Figure 2. Spectrum of Quartz-Tungsten halogen lamp used for polarimetry experiments. Data provided by National Institute of Standards and Technology. The vertical lines indicate the range of wavelengths visible to the human eye. Note that the lamp spectrum extends well into the infrared range.

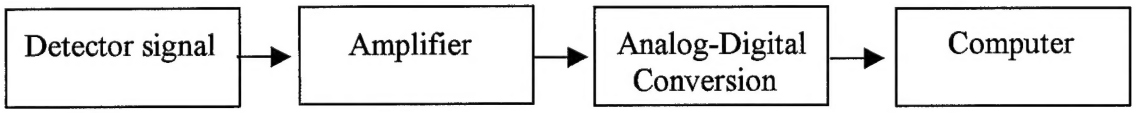

Figure 3. Chain of data acquisition for polarimetry experiments.

Film samples were generated from nearly all major brands of mammography film in use by mammography facilities in the United States. Pieces of film were exposed to controlled levels of ambient light to produce samples of a given optical density.

Results

A sample data set is shown in figure 4 for Min R E film (Eastman Kodak Co, Rochester, NY) at an optical density of near base+fog (no appreciable emulsion on the film). From the behavior of the resulting curves, strong retardance by the film is evident. At a certain angle between the optical axis of the sample S and that of P1 results in nearly a constant signal, suggesting that the sample behaves as a quarter-wave plate. If the sample were a perfect quarter wave plate, then one would observe a constant signal at an angle of 45 degrees between the

optical axis of the sample and that of P1, since at this angle the light transmitted by the sample would be circularly polarized. Rotation of P2 would therefore have no influence on the intensity of light reaching the detector. The fact that this is not so here (observe that the angle at which the signal possesses minimal variation is near 25 degrees), along with the observation that the signal never reaches zero indicates that other polarimetric properties of the film may be present. Strong dichroic properties appear to be minimal.

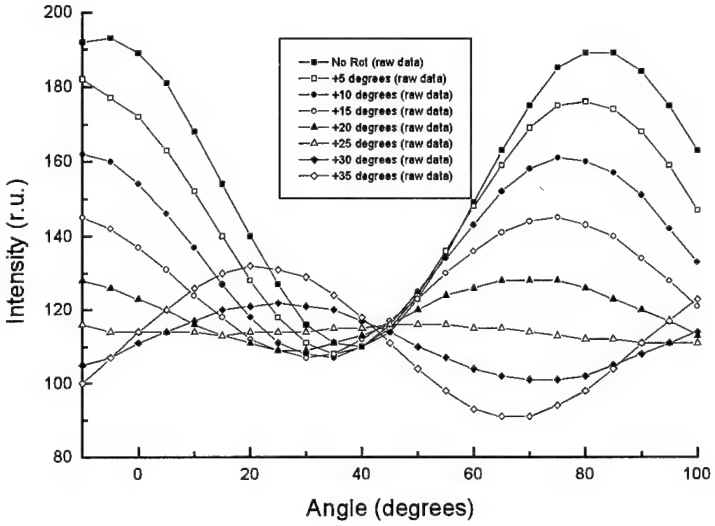

Figure 4. Illustration of P S P sample data for Min R E film at an optical density of near-base-plus-fog. The x-axis denotes rotation of polarizer P2, while successive curves denote increasing rotation of the film sample relative to P1.

One can readily observe these behaviors as well with two polarizers which sandwich a film sample. One polarizer is placed on a viewbox and then a film sample is placed over this polarizer. One then observes the film through a second, hand-held polarizer while the polarizer is rotated. Additionally rotating the film sample with respect to the first polarizer alters the relative orientation of the optical axes of the elements, as one can observe with the set-up described above.

Experiment: P C S C P Polarimetry

Purpose: To acquire data which will allow the determination of the Mueller Matrix for mammography films.

Procedure: The experimental configuration for mammography film polarimetry is shown in figure 5.

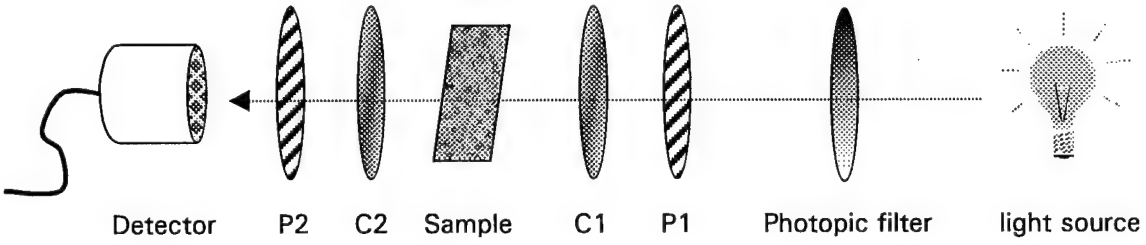

Figure 5. Optical set-up for the polarimetric measurements following the method of Azzam. Data analysis of the resulting optical signal allows complete determination of the Mueller Matrix.

The experiment utilizes two polarizers P1 and P2, two quarter-wave retarders C1 and C2, a light source and photodetector. A sample is placed between the retarders, and the retarders are then rotated through a given range of angles, with retarder C1 rotated in steps of θ and retarder C2 rotated in steps of 5θ. The film sample and polarizers P1 and P2 are kept stationary during the data acquisition. Temporal fluctuations in the output intensity of the light source were minimized by employing photofeedback. A micro-stepping motor was programmed to automate rotations of the retarders in conjunction with computer acquisition of the detector signal using an on-board analog-to-digital converter board. A total of 256 samples were taken to facilitate the use of fast-Fourier transform (FFT) techniques used in data analysis procedures, when used.

The light source used for this set of experiments was filtered with a photopic filter so as to shape the spectrum to match the sensitivity of the human eye. Figure 6 shows a plot of the spectral response of the photopic filter. The filter also effectively removed unwanted spectral components from the source, namely infrared. As the optical density of sample increased, it became necessary to increase gain on the photodetector amplifier to compensate for substantial reduction in light transmitted by the film sample. Dark current levels were measured for each amplifier gain stage in order to compensate for changes in the DC component of subsequent sample signals taken at different gain settings.

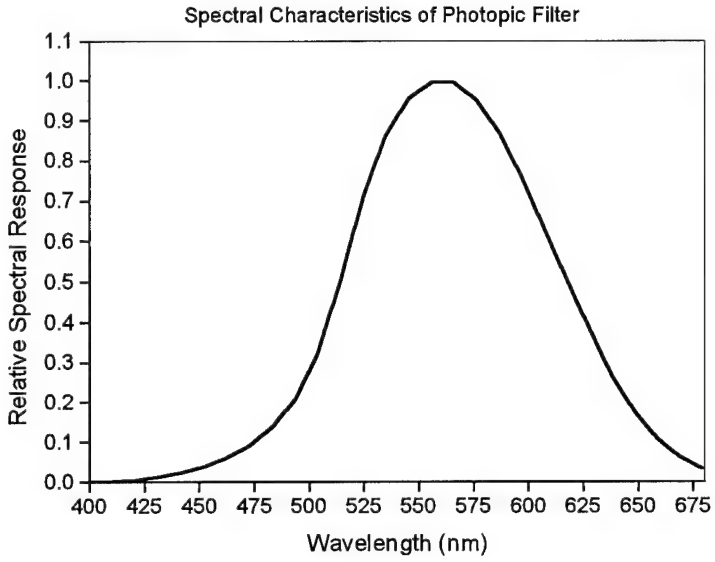

Figure 6. Spectral response of the photopic filter used with the P C S C P polarimeter.

Prior to acquiring data on mammography film samples the various optical elements of the polarimeter must be properly aligned. By taking data in the absence of a sample (air data), the polarimeter can be aligned from a knowledge of the optical polarimetric properties of air, which in effect yield a Mueller matrix equal to the identity matrix, $[M] = \delta_{ij}$.

Data was acquired for the following brands and types of mammography film:

Film Manufacturer	Film Types
Eastman Kodak Co.	Min R E, Min R 2000
Fuji	UM MA, UM MH
Agfa	MR-5
Dupont/Sterling	Microvision

These films represent the most popular film types in use currently by mammography facilities, according to 1997 MQSA inspection data from FDA's Division of Mammography Quality and Radiation Programs. Samples of each film type were made by exposing the film to successive levels of visible light. Optical densities investigated ranged from base+fog (B+F) level (essentially no emulsion on the film base) to approximately 3.5. Optical densities were measured with a Macbeth model TD-350 densitometer which had been calibrated to a NIST-traceable density strip. For each day on which data was acquired, air data was first acquired to account for slight differences in the source intensity, and to verify alignment of the optical elements. Each sample was positioned so that the apparent optical axis of the film aligned with that of the polarimeter. This ensured that all film samples of the same brand were positioned similarly.

The Mueller matrix is calculated according to the method of Azzam. Here the elements of the Mueller matrix are denoted by m_{ij} and the Fourier amplitudes for the cosine and sine terms of the detected signal are a_i and b_i, respectively. The relationships between the elements m_{ij} and the Fourier amplitudes of the detected signal are given by:

$$m_{24} = -4b_9$$
$$m_{34} = 4a_9$$
$$m_{44} = -2a_4$$
$$m_{43} = -4a_3$$
$$m_{42} = -4b_3$$

$$m_{22} = 4(a_8 + a_{12})$$
$$m_{23} = 4(b_{12} - b_8)$$
$$m_{32} = 4(b_8 + b_{12})$$
$$m_{33} = 4(a_8 - a_{12})$$

$$m_{12} = 2a_2 - \tfrac{1}{2} m_{22}$$
$$m_{21} = 2a_{10} - \tfrac{1}{2} m_{22}$$
$$m_{13} = 2b_2 - \tfrac{1}{2} m_{23}$$
$$m_{31} = 2b_{10} - \tfrac{1}{2} m_{32}$$
$$m_{11} = a_0 - \tfrac{1}{2} m_{12} - \tfrac{1}{2} m_{21} - \tfrac{1}{4} m_{22}$$

The Mueller matrix for a specific sample is then normalized with respect to m_{11} of the air data matrix generated from data measured earlier in the day.

Results: Air data.

Figure 7 shows a plot of air (no sample) data acquired from the polarimeter.

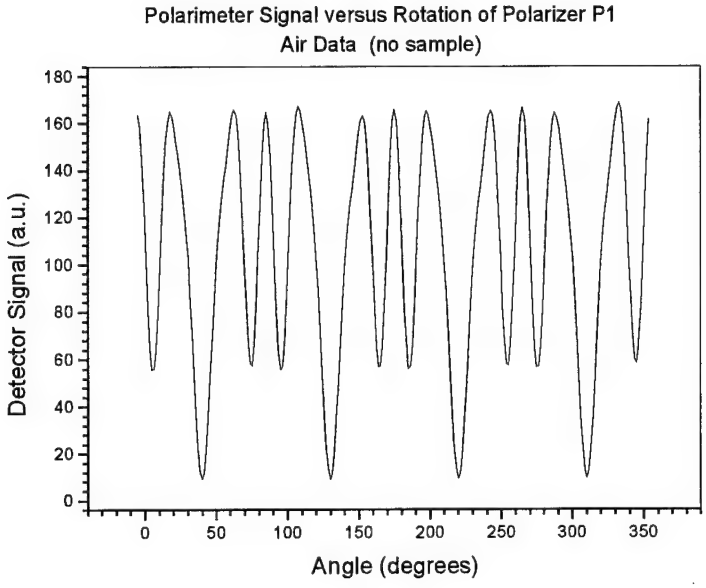

Figure 7. Plot of air data acquired with polarimeter. Air data was acquired each day that mammography film samples were analyzed.

A resulting Mueller matrix obtained from one polarimeter run taken on air was,

$$M_{air} = \begin{bmatrix} 1. & -0.0294547 & -0.0134345 & 0.00064046 \\ -0.0354645 & 1.00694 & 0.00530258 & -0.0016497 \\ -0.000836869 & -0.00408485 & 1.00539 & 0.00000923089 \\ 0.0001574 & -0.000354233 & 0.00178554 & 0.942315 \end{bmatrix}$$

Similar Mueller matrices resulted for further sets of air data. Matrices for air were normalized with respect to the m_{11} component.

Results: Computer Simulation

Software was written using the *Mathematica* scientific computing software package to model the output signal from the polarimeter and to compute Mueller matrices. As the Mueller matrices of the polarimeter components are ideally known, the Stokes vector for a incident state of light can be followed through the detector analytically, and the resulting transmission intensity computed. This aided in several important areas. Simple hypothetical experiments could be conducted quickly. Second, since the computer is capable of conducting experiments with 'perfect' optical elements, it aided in the isolation of errors occurring in the lab by comparison with experimental results. The software also permitted the computation of hypothetical transmission intensities from the polarimeter and corresponding Mueller matrices for samples which were unavailable or not realizable, such as a perfect quarter-wave retarder over a finite spectral range.

Four examples below (figures 8-11) illustrate the operation of the computer model. Shown are transmission intensities and resulting Fourier spectrum amplitudes for three configurations of samples:

- Air (no sample)
- Quarter-wave retarder
- Linear polarizer with optical axis aligned with polarimeter
- Linear polarizer with optical axis at 90 degrees with respect to polarimeter axis

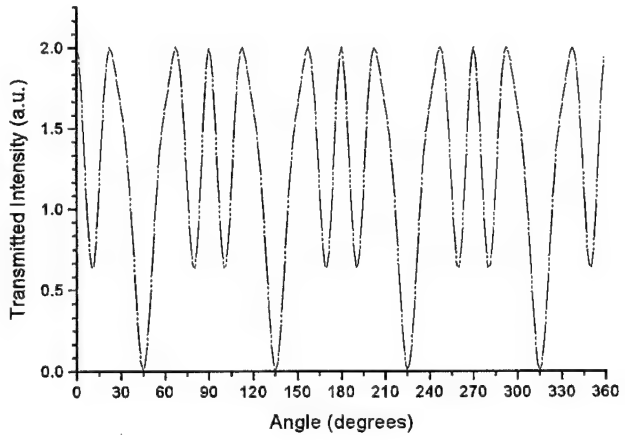

Figure 8. Results from computer modeling of polarimeter with no sample.

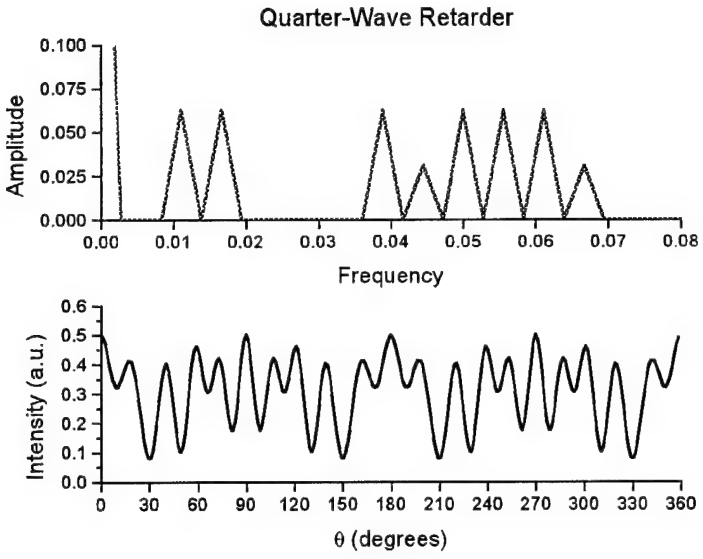

Figure 9. Results from computer modeling of polarimeter with quarter-wave retarder as the sample. Lower plot is transmitted intensity from the polarimeter. Upper plot shows the resulting Fourier spectrum components used to compute the Mueller matrix.

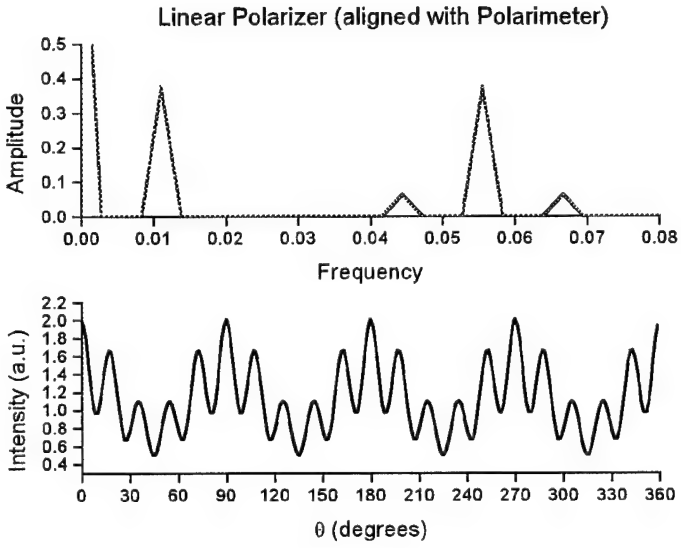

Figure 10. Computer simulation results for a linear polarizer with its optical axis aligned with that of the polarimeter. Bottom plot is transmitted intensity. Upper plot shows the resulting Fourier components used to compute the Mueller matrix.

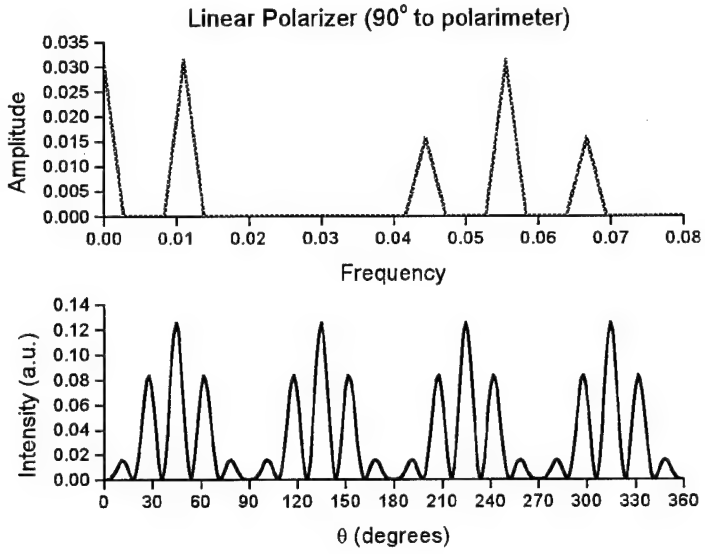

Figure 11. Computer simulation results for a linear polarizer with its optical axis oriented at 90 degrees with that of the polarimeter. Bottom plot is transmitted intensity. Upper plot shows the resulting Fourier components used to compute the Mueller matrix.

The Mueller matrices corresponding to the computer simulations presented above are as follows:

$$M_{air} = \begin{bmatrix} 1.0 & 0 & 0 & 0 \\ 0 & 1.0 & 0 & 0 \\ 0 & 0 & 1.0 & 0 \\ 0 & 0 & 0 & 1.0 \end{bmatrix}, \qquad M_{\substack{quarter-wave \\ retarder}} = \begin{bmatrix} 1.0 & 0 & 0 & 0 \\ 0 & 1.0 & 0 & 0 \\ 0 & 0 & 0 & -1.0 \\ 0 & 0 & 1.0 & 0 \end{bmatrix},$$

$$M_{\substack{linear\ polarizer \\ -\ aligned}} = \begin{bmatrix} 0.5 & 0.5 & 0 & 0 \\ 0.5 & 0.5 & 0 & 0 \\ 0 & 0 & 0 & 0 \\ 0 & 0 & 0 & 0 \end{bmatrix}, \quad \text{and} \quad M_{\substack{linear\ polarizer \\ 90\ deg}} = \begin{bmatrix} 0.5 & -0.5 & 0 & 0 \\ -0.5 & 0.5 & 0 & 0 \\ 0 & 0 & 0 & 0 \\ 0 & 0 & 0 & 0 \end{bmatrix}.$$

The ability of the computer simulations to also model aspects of a real polarimeter was of extreme value in accounting for observed measurements, and this utility will be discussed further below.

Mammography Film Data

Mammography film samples were studied over a range of optical densities from base-plus-fog level to approximately 3.5, roughly the limit of clinical usefulness. Figures 12-14 show sets of polarimeter signals for three brands of mammography film.

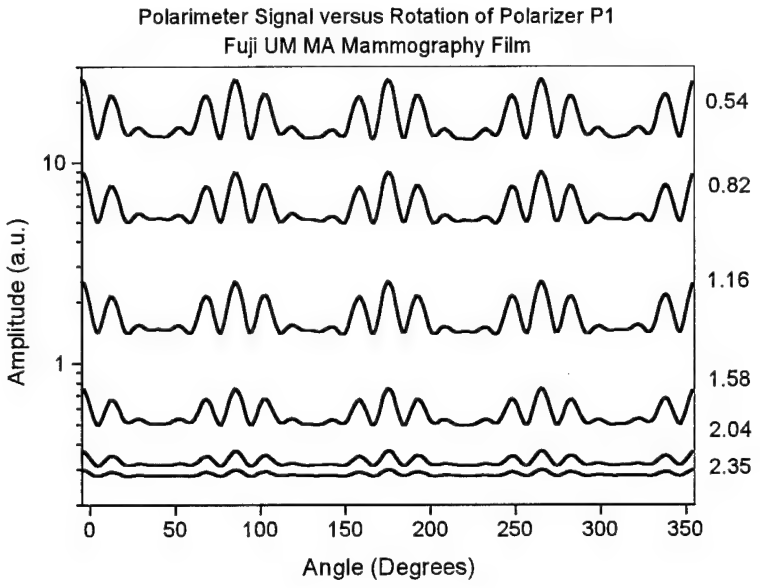

Figure 12. Polarimeter signals for Fuji UM MA mammography film. The succession of curves are for samples of optical density indicated along the right vertical axis.

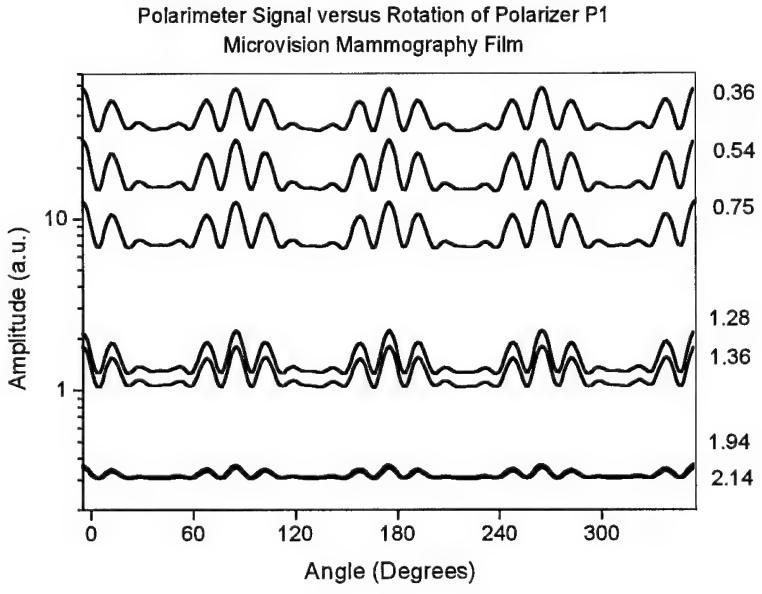

Figure 13. Polarimeter signals for Microvision mammography film. The succession of curves are for samples of optical density indicated along the right vertical axis.

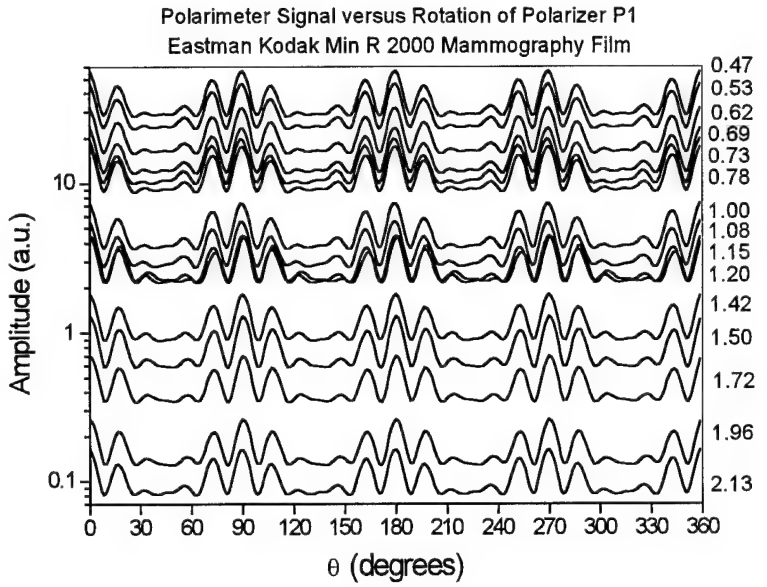

Figure 14. Polarimeter signals for Eastman Kodak Min R 2000 mammography film. The succession of curves are for samples of optical density indicated along the right vertical axis.

Corresponding Mueller matrices for the case of Eastman Kodak Min R E film are given below. Each of the Mueller matrices was scaled by m_{11} from the Mueller matrix for air.

OD=0.00 (air)

$$\begin{pmatrix} 1.000 & -0.029 & -0.007 & 0.002 \\ -0.036 & 0.982 & 0.028 & -0.000 \\ 0.014 & -0.024 & 0.979 & 0.000 \\ -0.002 & -0.003 & 0.002 & 0.918 \end{pmatrix}$$

OD 0.20 (base+fog)

$$\begin{pmatrix} 0.504 & -0.013 & 0.000 & 0.000 \\ -0.016 & 0.527 & 0.015 & 0.005 \\ 0.003 & -0.056 & 0.000 & 0.008 \\ 0.015 & 0.016 & -0.006 & 0.000 \end{pmatrix}$$

OD 1.35

$$\begin{pmatrix} 0.490 & -0.009 & 0.003 & 0.000 \\ -0.020 & 0.528 & 0.033 & 0.021 \\ -0.004 & -0.005 & 0.006 & 0.001 \\ -0.011 & -0.013 & -0.004 & 0.000 \end{pmatrix} \times 10^{-2}$$

OD 1.49

$$\begin{pmatrix} 0.292 & -0.004 & 0.002 & 0.001 \\ -0.012 & 0.316 & 0.027 & 0.012 \\ -0.003 & 0.008 & 0.005 & 0.002 \\ -0.008 & -0.010 & -0.003 & 0.000 \end{pmatrix} \times 10^{-2}$$

OD 1.69

$$\begin{pmatrix} 0.151 & -0.004 & 0.001 & 0.001 \\ -0.006 & 0.160 & 0.010 & -0.001 \\ 0.000 & -0.007 & 0.000 & 0.001 \\ 0.005 & 0.005 & 0.000 & 0.000 \end{pmatrix} \times 10^{-2}$$

OD 1.91

$$\begin{pmatrix} 0.673 & -0.018 & -0.001 & 0.000 \\ -0.022 & 0.694 & 0.010 & -0.004 \\ 0.007 & -0.113 & -0.003 & 0.000 \\ 0.039 & 0.040 & 0.001 & 0.002 \end{pmatrix} \times 10^{-3}$$

OD 2.03

$$\begin{pmatrix} 0.445 & -0.011 & 0.006 & 0.004 \\ -0.016 & 0.467 & 0.037 & -0.002 \\ 0.001 & -0.019 & 0.000 & 0.002 \\ 0.015 & 0.014 & 0.000 & 0.001 \end{pmatrix} \times 10^{-3}$$

OD 2.22

$$\begin{pmatrix} 0.228 & -0.006 & -0.001 & 0.000 \\ -0.007 & 0.227 & 0.073 & -0.001 \\ -0.002 & 0.047 & 0.016 & 0.000 \\ 0.008 & 0.008 & 0.002 & 0.000 \end{pmatrix} \times 10^{-3}$$

OD 2.26

$$\begin{pmatrix} 0.200 & -0.006 & 0.002 & 0.002 \\ -0.007 & 0.205 & 0.055 & -0.001 \\ -0.001 & 0.032 & 0.009 & 0.001 \\ 0.006 & 0.005 & 0.002 & 0.000 \end{pmatrix} \times 10^{-3}$$

OD 2.43

$$\begin{pmatrix} 0.115 & -0.003 & 0.000 & 0.000 \\ -0.004 & 0.112 & 0.042 & 0.006 \\ -0.001 & 0.027 & 0.010 & 0.002 \\ -0.002 & -0.002 & -0.001 & 0.000 \end{pmatrix} \times 10^{-3}$$

OD 2.55

$$\begin{pmatrix} 0.829 & -0.023 & 0.009 & 0.006 \\ -0.029 & 0.877 & 0.102 & 0.047 \\ 0.005 & -0.029 & -0.004 & 0.002 \\ -0.011 & -0.013 & -0.003 & 0.000 \end{pmatrix} \times 10^{-4}$$

OD 2.73

$$\begin{pmatrix} 0.457 & -0.012 & 0.006 & 0.002 \\ -0.018 & 0.493 & 0.022 & 0.023 \\ 0.002 & -0.032 & -0.001 & 0.001 \\ -0.008 & -0.010 & -0.003 & -0.002 \end{pmatrix} \times 10^{-4}$$

OD 2.78

$$\begin{pmatrix} 0.342 & -0.008 & 0.002 & 0.001 \\ -0.015 & 0.377 & 0.016 & -0.002 \\ -0.001 & -0.022 & 0.003 & 0.003 \\ 0.012 & 0.011 & -0.002 & 0.000 \end{pmatrix} \times 10^{-4}$$

OD 2.95

$$\begin{pmatrix} 0.194 & -0.005 & 0.001 & 0.001 \\ -0.008 & 0.216 & 0.027 & -0.002 \\ -0.001 & 0.007 & 0.002 & 0.001 \\ 0.006 & 0.006 & 0.000 & 0.000 \end{pmatrix} \times 10^{-4}$$

OD 3.07

$$\begin{pmatrix} 0.141 & -0.002 & 0.001 & 0.001 \\ -0.006 & 0.159 & 0.005 & 0.007 \\ 0.000 & -0.010 & 0.001 & 0.000 \\ -0.003 & -0.004 & -0.002 & 0.000 \end{pmatrix} \times 10^{-4}$$

OD 3.10

$$\begin{pmatrix} 0.124 & -0.002 & 0.001 & 0.000 \\ -0.005 & 0.139 & 0.020 & 0.006 \\ -0.001 & 0.011 & 0.003 & 0.002 \\ -0.003 & -0.004 & -0.002 & -0.001 \end{pmatrix} \times 10^{-4}$$

OD 3.15

$$\begin{pmatrix} 0.097 & -0.003 & -0.001 & 0.000 \\ -0.004 & 0.107 & 0.026 & -0.001 \\ 0.000 & 0.015 & 0.005 & 0.000 \\ 0.004 & 0.005 & 0.000 & 0.000 \end{pmatrix} \times 10^{-4}$$

OD 3.28

$$\begin{pmatrix} 0.676 & -0.021 & 0.004 & 0.000 \\ -0.030 & 0.681 & 0.240 & 0.000 \\ -0.013 & 0.178 & 0.078 & 0.006 \\ 0.020 & 0.016 & 0.010 & 0.000 \end{pmatrix} \times 10^{-5}$$

OD 3.34

$$\begin{pmatrix} 0.574 & -0.008 & -0.002 & 0.008 \\ -0.020 & 0.521 & 0.203 & -0.010 \\ -0.012 & 0.169 & 0.071 & 0.006 \\ 0.006 & -0.002 & 0.001 & -0.002 \end{pmatrix} \times 10^{-5}$$

OD 3.42

$$\begin{pmatrix} 0.440 & -0.004 & 0.001 & 0.003 \\ -0.017 & 0.329 & 0.124 & 0.007 \\ -0.011 & 0.122 & 0.049 & 0.009 \\ -0.014 & -0.017 & -0.003 & -0.001 \end{pmatrix} \times 10^{-5}$$

OD 3.51

$$\begin{pmatrix} 0.408 & 0.000 & 0.004 & 0.003 \\ -0.004 & 0.216 & 0.136 & -0.002 \\ -0.003 & 0.125 & 0.075 & 0.000 \\ 0.006 & 0.006 & 0.003 & -0.002 \end{pmatrix} \times 10^{-5}$$

OD 3.55

$$\begin{pmatrix} 0.398 & -0.006 & 0.001 & 0.001 \\ -0.015 & 0.296 & 0.047 & 0.011 \\ -0.001 & 0.034 & 0.012 & 0.003 \\ -0.008 & -0.011 & -0.004 & 0.001 \end{pmatrix} \times 10^{-5}$$

OD 3.67

$$\begin{pmatrix} 0.334 & -0.005 & 0.001 & 0.002 \\ -0.004 & 0.208 & 0.063 & 0.010 \\ 0.000 & 0.031 & 0.014 & 0.002 \\ 0.002 & 0.002 & 0.001 & 0.003 \end{pmatrix} \times 10^{-5}$$

OD 3.77

$$\begin{pmatrix} 0.274 & -0.003 & -0.004 & 0.000 \\ -0.005 & 0.153 & 0.026 & 0.004 \\ -0.001 & 0.014 & 0.005 & 0.003 \\ -0.002 & -0.004 & 0.005 & 0.001 \end{pmatrix} \times 10^{-5}$$

The Mueller matrix for each film brand and type was found to have the same general form,

$$M = \begin{bmatrix} \alpha & 0 & 0 & 0 \\ 0 & \beta & 0 & 0 \\ 0 & 0 & 0 & 0 \\ 0 & 0 & 0 & 0 \end{bmatrix}$$

over the entire range of clinically useful optical densities. The primary objective of the project was to determine whether any relationship exists between mammography film density and polarimetric behavior by the film. The dependence of the Mueller matrix on optical density was thus expressed by examining the ratio of the two Mueller matrix elements m_{22}/m_{11}, or β/α. In the form above, the term α essentially determines the transmission of the film sample, while the term β reflects the extent to which the sample influences the polarimetric properties of an incident beam of light. To understand the influence of the term β on the state of polarization of transmitted light, let β approach zero. We would then have, for an incident beam of any form and degree of polarization,

$$\begin{bmatrix} S_0' \\ S_1' \\ S_2' \\ S_3' \end{bmatrix} = \begin{bmatrix} \alpha & 0 & 0 & 0 \\ 0 & 0 & 0 & 0 \\ 0 & 0 & 0 & 0 \\ 0 & 0 & 0 & 0 \end{bmatrix} \begin{bmatrix} S_0 \\ S_1 \\ S_2 \\ S_3 \end{bmatrix} = \alpha S_0 \cdot \begin{bmatrix} 1 \\ 0 \\ 0 \\ 0 \end{bmatrix}.$$

This is the Stokes vector for completely unpolarized light, scaled by the factor α. Hence in this case the sample would behave as a perfect depolarizer. Since in general

$$S_0^2 \geq S_1^2 + S_2^2 + S_3^2 ,$$

this restricts β to values which do not exceed that of α. Mueller matrices were computed from polarimetry data taken on samples of mammography films, and values for β / α were computed. Plots of β / α for the brands and types of films studied are given in figures 15-18.

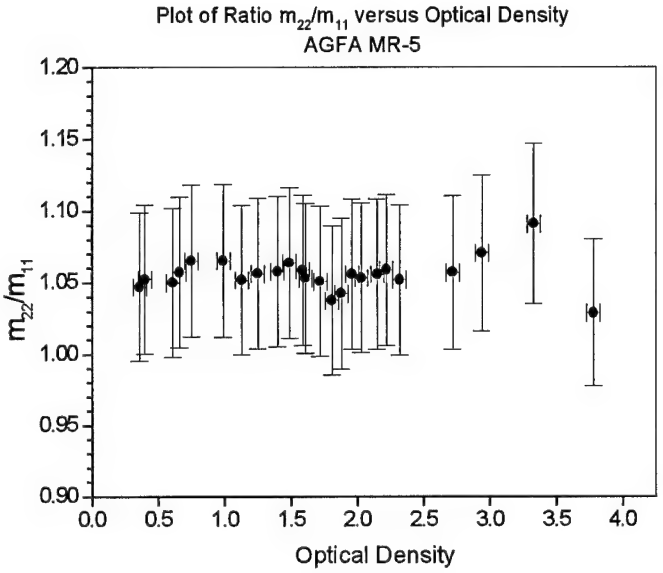

Figure 15. Plot of the ratio of the Mueller matrix elements m_{22}/m_{11} versus optical density for AGFA MR-5 mammography film.

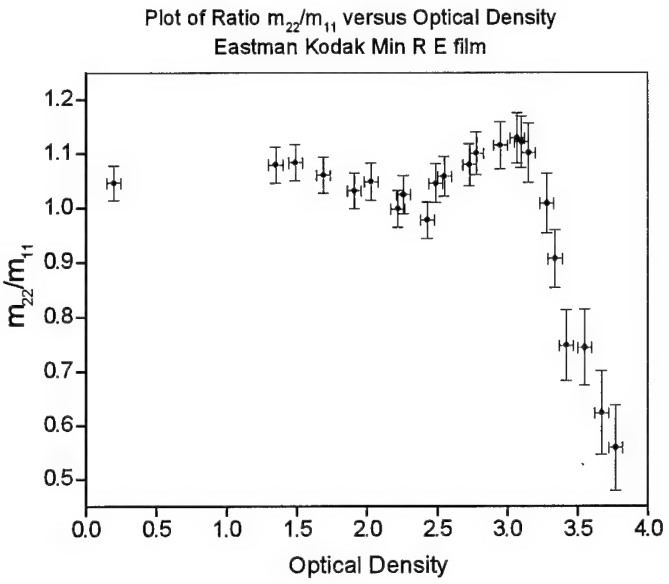

Figure 16. Plot of the ratio of the Mueller matrix elements m_{22}/m_{11} versus optical density for Eastman Kodak Min R E mammography film.

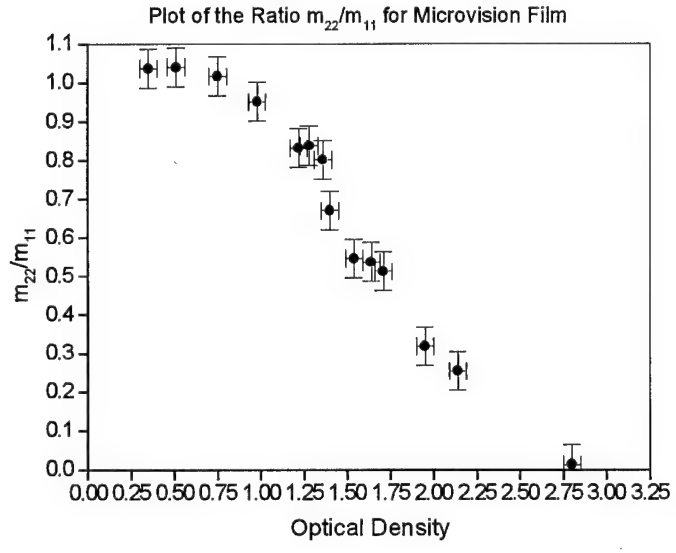

Figure 17. Plot of the ratio of the Mueller matrix elements m_{22}/m_{11} versus optical density for Sterling Microvision mammography film.

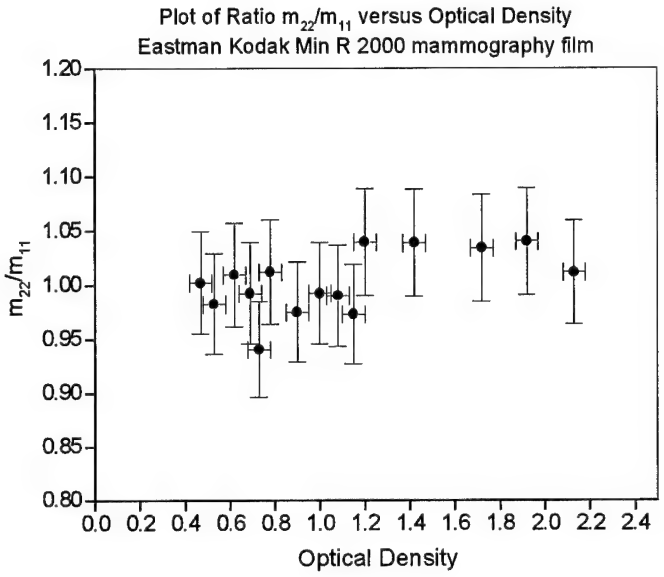

Figure 18. Plot of the ratio of the Mueller matrix elements m_{22}/m_{11} versus optical density for Eastman Kodak Min R 2000 mammography film.

Discussion

In most all cases, the ratio β/α ($= m_{22}/m_{11}$) remains nearly constant across the range of optical densities. Some of the film samples also resulted in a drop in β/α with increasing optical density as illustrated by the plots for Microvision and Min R E films. The validity of this trend was tested further and is discussed below. Films showing this trend were earlier sets of data taken on the polarimeter, and the source of this behavior was eventually traced to reduced signal-noise ratios at high optical densities. Hence, subsequent data taken on the polarimeter produced no significant trend in β/α with optical density, as shown for the case of Agfa MR mammography film in figure 15. It should be noted that the ratios plotted above show values for β/α exceeding one. Possible sources of this error are also investigated below. The data nonetheless indicates a lack of a strong relationship of optical polarimetric properties with optical density. This further supports the contention that the polarimetric properties of the base of the film are the dominant factor.

Error Analysis

An attempt was made to correct for errors in the Mueller matrices for air data following the method of Goldstein and Chipman[3]. This publication outlines errors one would observe in the

Mueller matrix for air if the polarimeter possessed certain types and degrees of misalignment of the optical components. It also specified corrections to the matrix elements provided that the exact nature of misalignment was identified. We were unable to significantly reduce errors in the Mueller matrices for air by following this method. We opted then to enforce strict alignment on the polarimeter, and were thus able to reduce errors in the Mueller matrix for air to our satisfaction.

A source of error that manifested itself for samples having high optical densities was a reduced signal-noise ratio. Since optical density is a logarithmic relationship with intensity, high optical densities can result in a reduction in transmitted intensity by an order of magnitude or greater compared with lower densities (note the range of the vertical axis on the plot in figure 14). Stray light sources can also become a source of error. Simply coupling the detector to the output of the analyzing polarizer P2 with a hollow tube significantly improved the quality of data in further experiments. The need to switch to higher gains on the amplifier as signal levels dropped was also compensated for by measuring dark currents at each gain setting. This removed bumps in the data occurring at points where gain levels were different.

Several sources of error are also possible in the optics of the polarimeter itself. First, errors could occur because of inferior quality of the polarimeter optics. Glan-Thompson polarizers were selected above dichroic sheet elements for their superior quality. Also, commercially available retarders generally have retardance which is dependent on wavelength. Figure 19 shows the manufacturer's specifications for the two retarders obtained for the polarimetry experiments. Overall, there is roughly a 4% deviation from ideal quarter-wave retardance. Computer simulations performed to model the non-perfect behavior of the quarter-wave retarders (discussed below) showed that this spectral dependence is not insignificant.

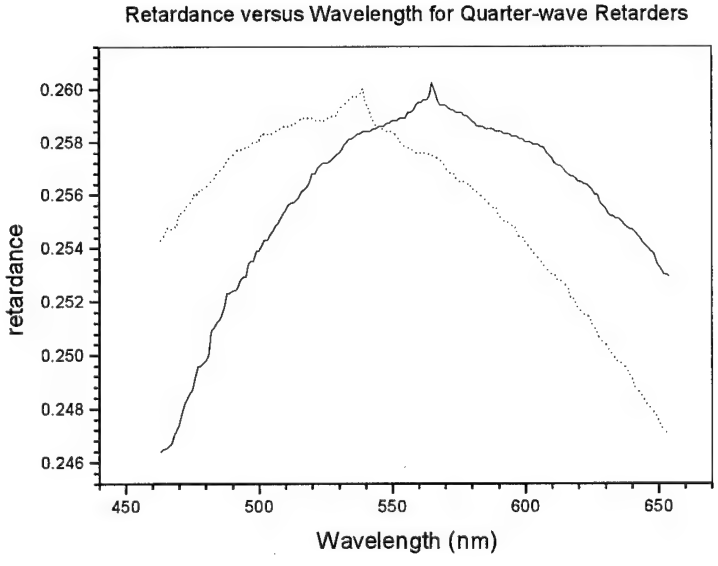

Figure 19. Dependence of retardance on wavelength for the quarter-wave retarders used in all polarimetry experiments. Note that not only is there variation over the visible spectrum, but also that due to variations in the manufacturing process, the values do not

Error can also occur because of azimuthal misalignment of the components. In other words, one or more elements would start off rotated by an arbitrary number of degrees relative to its proper orientation. Periodically the polarimeter was realigned to ensure minimal effects of this type of error. Air data taken each day served also to verify that the polarimeter was aligned as best possible.

Finally, long term modulation of the signal (such as perhaps slight drift in the source light output) can introduce error into subsequent calculations.

In order to better understand the influence of various sources of error on the results, a comparison was performed of measured signal data to corresponding data generated by computer simulation. Modification to sets of ideal (perfect) polarimeter data was done to computer model the influence of the following sources of error:

1. azimuthal misalignment
2. imperfect quarter-wave retardance over relevant source spectrum
3. slight modulation of signal amplitude during course of a sample run
4. the presence of noise

An ideal Mueller matrix was used for a film sample, having $m_{11}=m_{22} = 1.0$ and all other elements equal to zero. Signal values corresponding to a polarimeter having the above listed sources of error were then generated. The simulated data were then used to generate corresponding Mueller matrices and then compared to Mueller matrices from experimental data.

Results

The result for a simulation of air data is given in figure 20. Comparison with the corresponding experimental results given in figure 7 shows quite good agreement.

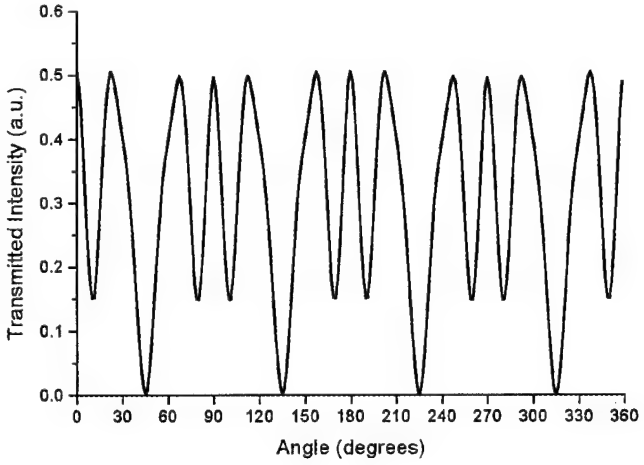

Figure 20. Simulated polarimeter signal for the case of air data.

The Mueller matrix resulting from this simulation for air is,

$$M_{air,simulated} = \begin{bmatrix} 1.00028 & -0.0466181 & 2.74884 \cdot 10^{-4} & -7.81634 \cdot 10^{-6} \\ -0.0299182 & 1.07302 & -9.31701 \cdot 10^{-4} & 5.17339 \cdot 10^{-4} \\ -7.62987 \cdot 10^{-5} & 3.3429 \cdot 10^{-4} & 1.07224 & 2.48877 \cdot 10^{-3} \\ 1.01061 \cdot 10^{-4} & 2.7467 \cdot 10^{-4} & 0.010119 & 0.995243 \end{bmatrix}.$$

With the initial assumption (input for the simulation) of the Mueller matrix for a film as having the structure,

$$M_{film,ideal} = \begin{bmatrix} 1 & 0 & 0 & 0 \\ 0 & 1 & 0 & 0 \\ 0 & 0 & 0 & 0 \\ 0 & 0 & 0 & 0 \end{bmatrix},$$

the simulation resulted in the error-adjusted Mueller matrix for a film,

$$M_{\substack{film,\,error\\adjusted}} = \begin{bmatrix} 1.0103 & -0.0460 & 0.0004 & 0.0001 \\ -0.0313 & 1.0714 & 0.0720 & -0.0008 \\ 0.0014 & -0.0810 & -0.0038 & -0.0009 \\ 0.0003 & -0.0001 & -0.0005 & -0.0015 \end{bmatrix}.$$

The resulting ratio of m_{22}/m_{11} is 1.06. This value is in good agreement with ratios observed from much of the data collected. The computer model therefore shows that ratios of m_{22}/m_{11} greater than zero can be expected with the experimental polarimeter, and validates the assumption as to the sources of this error.

Experiment: P S P Polarimetry for the determination of the ratio β/α.

Procedure: The P S P experiment discussed above was repeated in order to validate the results of the Mueller matrix polarimetry. Specifically, it was sought to validate that the films investigated possess a very weak optical polarimetric relationship with optical density, and that the Mueller matrices for these films are essentially contained in the values of m_{11} and m_{22}.

If the films possess a Mueller matrix of the form,

$$M = \begin{bmatrix} \alpha & 0 & 0 & 0 \\ 0 & \beta & 0 & 0 \\ 0 & 0 & 0 & 0 \\ 0 & 0 & 0 & 0 \end{bmatrix},$$

then the predicted signal reaching the detector for the P S P polarimeter has the general form,

$$S(\theta) = \tfrac{1}{4}\left[\alpha + \beta \cdot \cos(2\theta)\right].$$

In the above expression the parameter θ specifies the angle of displacement of polarizer P1. The parameters α and β can then be determined directly from the measured signals.

Film samples were positioned with their optical axes aligned with that of the polarizers. Subsequent data was taken in sufficient amount to cover at least one complete cycle. Figure 21 shows samples signals acquired on Agfa MR 5 film, and Figures 22 through 26 give values of m_{11}, m_{22} and the ratio m_{22}/m_{11} ($=\beta/\alpha$) obtained for all films investigated. Data taken at high optical densities had acceptable levels of signal-noise ratio, and dark current levels for each gain setting were again accounted for prior to analyzing the data.

The data confirm the results of the Mueller matrix polarimetry of the previous section. Specifically, the results confirm that the ratio m_{22}/m_{11} is essentially a constant value across the entire range of clinically useful optical densities, and thus the mammography films tested display no relevant optical polarimetric properties which are determined by the level of optical density.

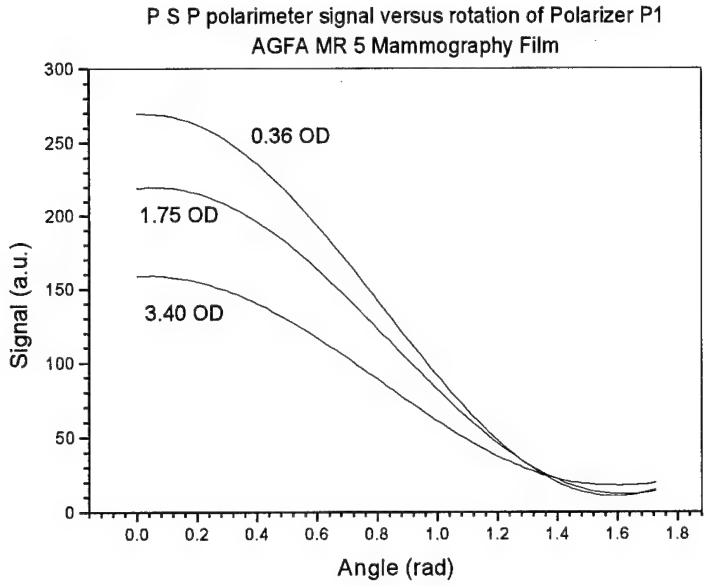

Figure 21. Plot of *PSP* polarimeter signal for several optical densities of Agfa MR 5 mammography film.

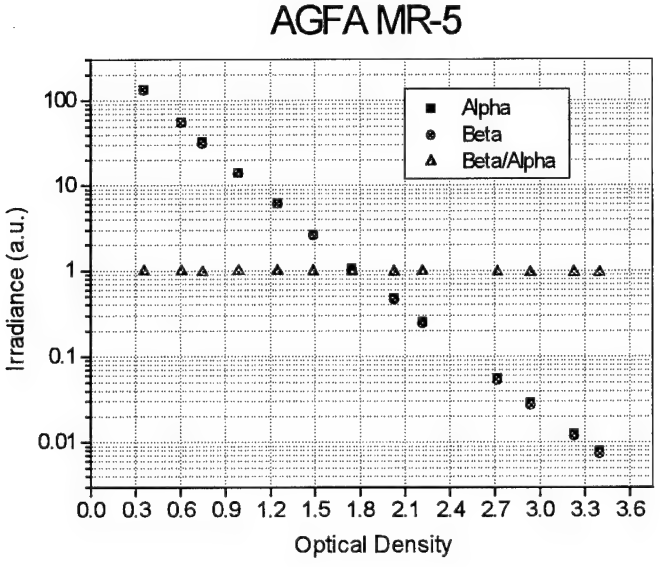

Figure 22. Plot of the Mueller matrix elements m_{11} (=alpha, α), m_{22} (=beta, β), and the ratio of m_{22}/m_{11} ($=\beta/\alpha$) versus optical density for Agfa MR 5 mammography film.

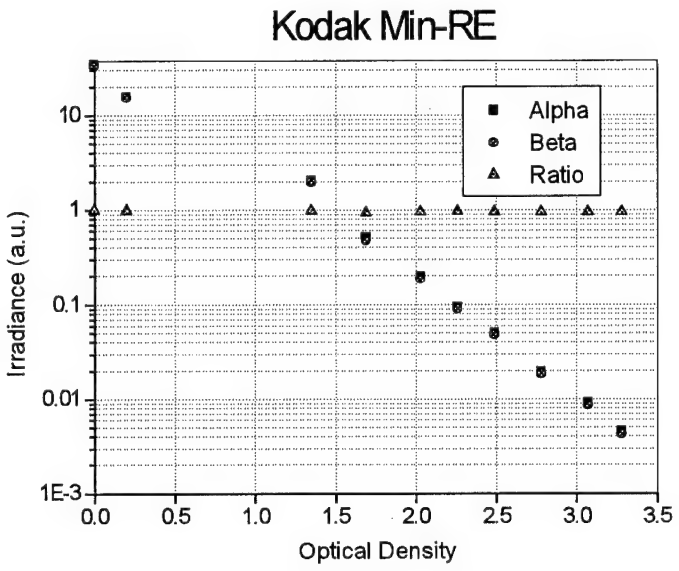

Figure 23. Plot of the Mueller matrix elements m_{11} ($=\alpha$), m_{22} ($=\beta$), and the ratio of m_{22}/m_{11} ($=\beta/\alpha$) versus optical density for Kodak Min R E mammography film.

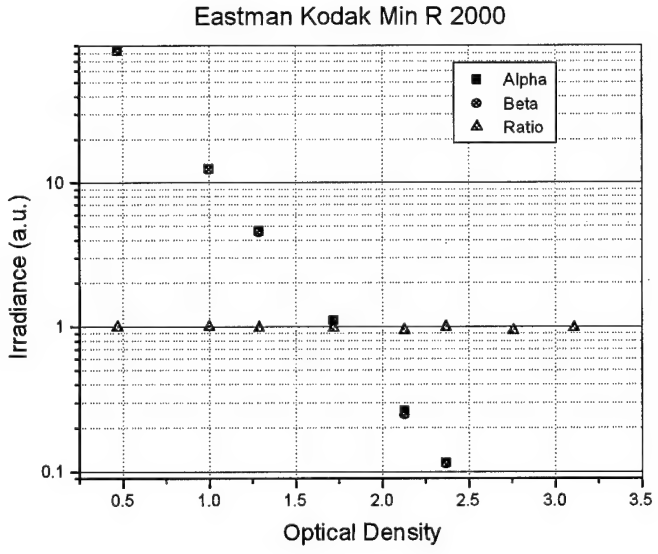

Figure 24. Plot of the Mueller matrix elements m_{11} ($=\alpha$), m_{22} ($=\beta$), and the ratio of m_{22}/m_{11} ($=\beta/\alpha$) versus optical density for Kodak Min R 2000 mammography film.

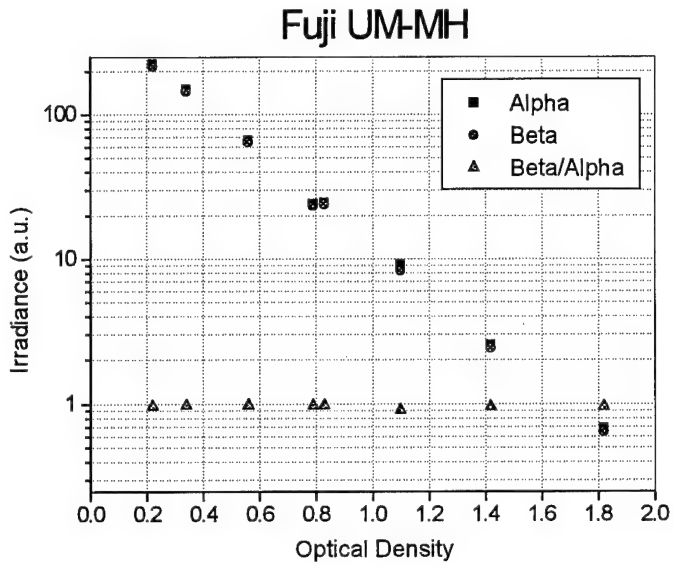

Figure 25. Plot of the Mueller matrix elements m_{11} ($=\alpha$), m_{22} ($=\beta$), and the ratio of m_{22}/m_{11} ($=\beta/\alpha$) versus optical density for Fuji UM-MH mammography film.

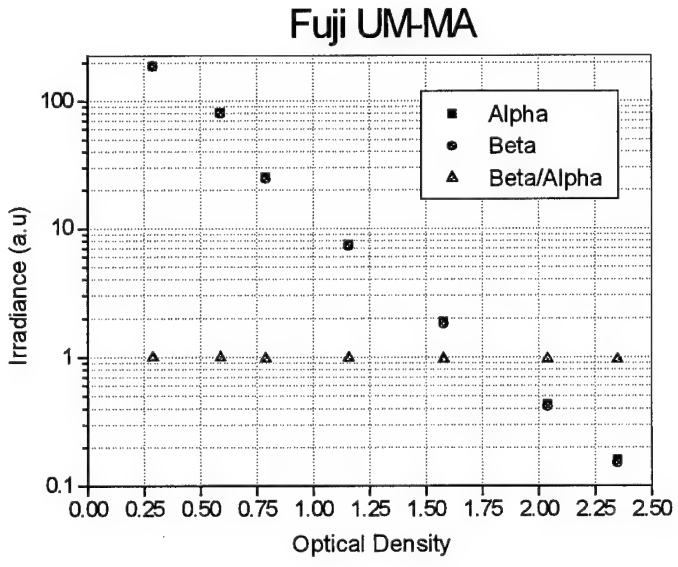

Figure 26. Plot of the Mueller matrix elements m_{11} ($=\alpha$), m_{22} ($=\beta$), and the ratio of m_{22}/m_{11} ($=\beta/\alpha$) versus optical density for Fuji UM-MA mammography film.

Experiment: Development and evaluation of prototype viewing device

Procedure: A template was developed for use with a conventional viewbox which utilizes two linear polarizers: one polarizer (P1) is placed between the viewbox panel (light source) and the film to be observed, and the second polarizer (P2, called the analyzer) is placed between the film and the observer. Figure 27 illustrates the geometry of this prototype.

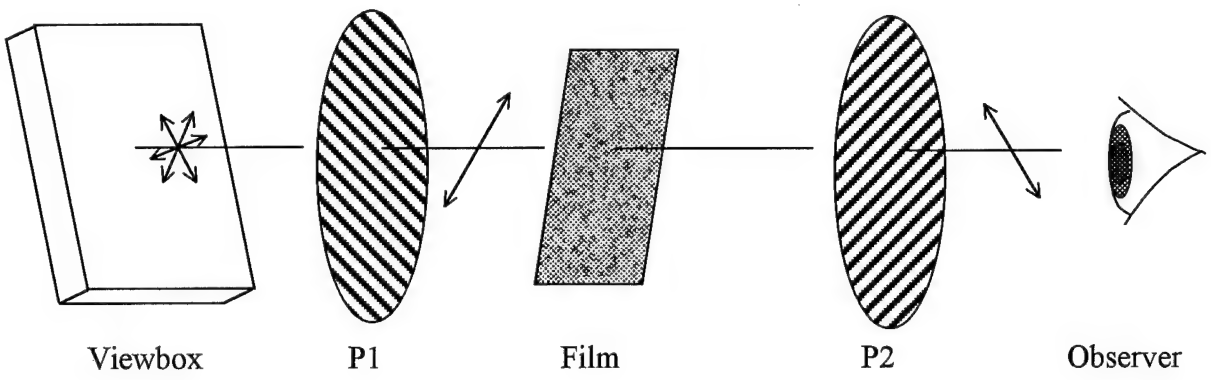

Figure 27. Diagram of prototype viewing template evaluated. Shown is an exploded view; the actual working device incorporated the polarizer P1 at the viewbox beneath the film being observed. The analyzing polarizer P2 was hand-held.

In this configuration, the film and polarizer P1 are held stationary while the observer views the resulting image through P2 as it is rotated. Once a desirable image is obtained, P2 can then be held stationary. It is possible for the optical axes of the film and the polarizer P1 to be such that when P2 is rotated, a minimal resulting change in the viewed image occurs. Hence prior to using the template to view mammograms, the orientation of the film with polarizer P1 needed to be adjusted. To do this the observer would place a film on the viewbox directly over P1. Next, while observing the film through the hand-held analyzer P2, polarizer P1 would be adjusted (rotated) such that the optical axes of the film and that of the polarizer P1 were aligned. This alignment would allow for the greatest range of 'viewed' densities when P2 was subsequently rotated.

To evaluate the effect of the prototype template on image quality as seen by the observer, a series of test films were generated covering a range of background densities, features and levels of image quality. An anthropomorphic mammography phantom containing a series of test objects was used to generate a series of films having a range of optical densities. Clinical films were also evaluated to test the ability of the prototype to improve the poor image quality of a mammogram. The investigators wish to emphasize strongly that *in no case* were mammograms obtained from patients strictly for the purpose of performing this evaluation. Only previously existing clinical films were used.

Two radiologists were asked to evaluate the prototype template. A demonstration was provided of the procedure for aligning the films with the polarizers after which each radiologist was given

a form with which to record their observations, a set of films and the template. The evaluation asked that each observer first evaluate the film on a standard viewbox without the prototype in order to determine initial level of quality in terms of acceptable background density and overall acceptability (if applicable, such as with the clinical films). Next both radiologists were asked to view the same film with the prototype and determine to what extent if any, it improved the perceived level of image quality compared to that observed with only a viewbox. Specific questions were asked regarding the following parameters:

- The type of feature(s) observed on the film:

  a. Microcalcification-like features
  b. Fibrous structures
  c. Masses

- The change in the relative contrast of the feature with the immediate background region.

- Any apparent changes in background clutter (undesirable surrounding regions of significant contrast) on the image.

- Any influence on the perceived sharpness of the feature.

- Overall improvement in diagnostic value over that obtained with the viewbox-only environment.

Responses were recorded on a scale of 1 (= much worse) to 5(= very much improved). If a particular film had more than one feature of interest on it, a separate set of responses were recorded for each feature. The viewbox was masked down so that only the relevant area of film was illuminated.

Results

Figure 28 shows a distribution of reported scores from both radiologists for the category of 'Overall Diagnostic Value' when compared with the same image prior to using the prototype template. The scores are distributed over a scale of 1 (= much worse) to 5(= much improved). For approximately 85 percent of the time the prototype device either rendered an image of the same level of quality (Reported Score = '3'), or resulted in a image of less diagnostic value than that observed without the template.

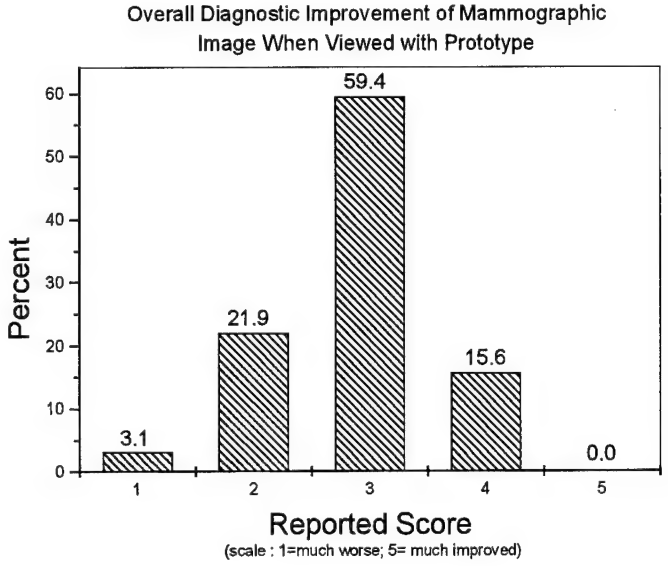

Figure 28. Distribution of reported scores for Overall Diagnostic Value for both readers.

Figure 29 shows a distribution of the assessment of specific aspects of image quality. Reported scores are shown for the relative effect the prototype device had on feature contrast with background, sharpness of the edges of features, and the influence of background structures (clutter) on the evaluation of features on the image. Sharpness of the edges of features was impacted the least of the three categories, while contrast with the background showed the most improvement, with nearly 30 percent with a score of '4'. No scores, however, were reported for 'much improved' (corresponding to a score of '5') for any of the image quality categories.

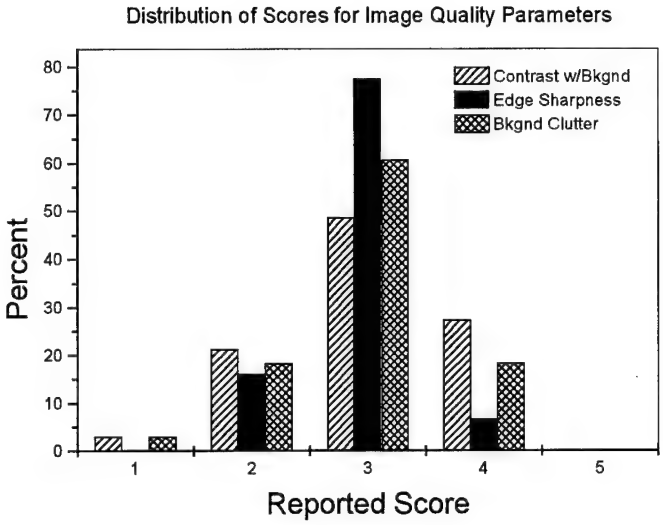

Figure 29. Distribution of reported scores for specific aspects of image quality influenced by the use of the prototype template. Scores are again reported on the scale of 1 (= much worse) to 5 (=much improved)

If the reported scores are broken down additionally by whether the initial review of the film found the background density to be either acceptable or too low (the film appears too light), then the scores show that the prototype was of more benefit to films having a lower background density than acceptable (Figure 30). Without regard to any polarimetric behavior by the film, this seems reasonable since one effect the polarizers have is a reduction in transmitted intensity to the viewer. Merely reducing the intensity of films that appear as too bright on a viewbox may have beneficial effects.

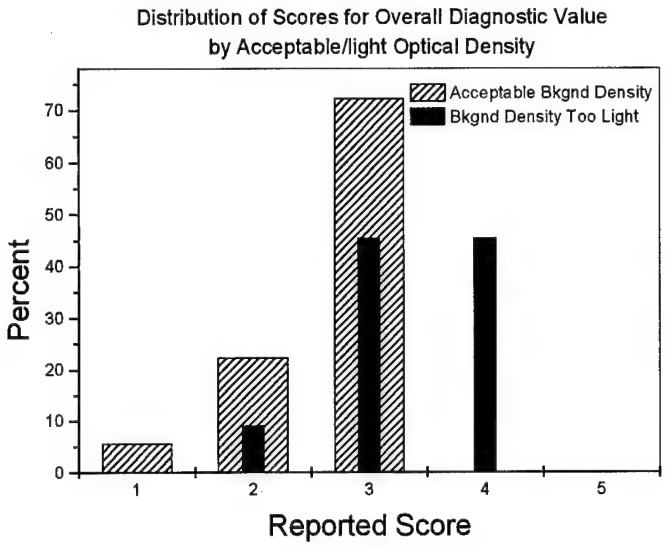

Figure 30. Distribution of reported scores for 'Overall Diagnostic Value' for the cases of films having acceptable background optical densities, and for films having lower background densities than acceptable.

Figures 31 and 32 show that there was benefit specifically to the appearance of contrast and reduction of background clutter for films having lower optical densities than acceptable. Given the results of the polarimetry studies of mammography films which show that there is no prominent optical polarimetric relationship with film optical density, it is difficult to conclude that these reported results are due to a definite polarimetric influence on the mammography film's image quality by the prototype device. The response of the human eye is such that films of low background optical density may saturate the eye's ability to respond to features on the film image. Hence the results above may be a result of the polarizers reducing the overall level of ambient light to a more comfortable level for the readers.

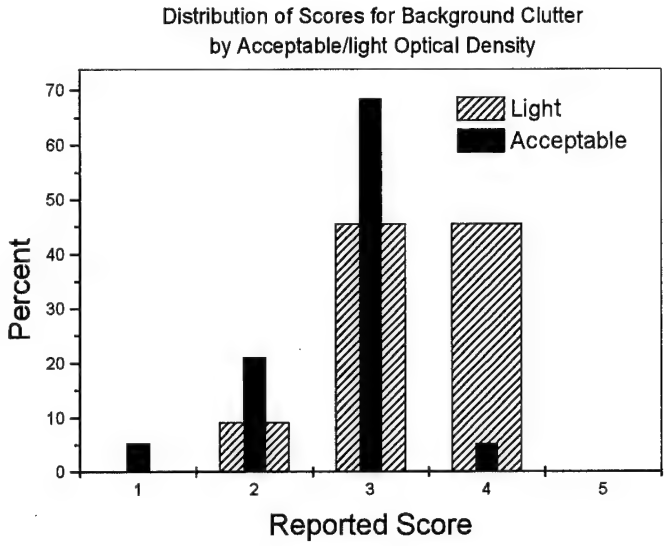

Figure 31. Distribution of reported scores for feature contrast for the cases of films having acceptable background density and for films having background density lower than acceptable.

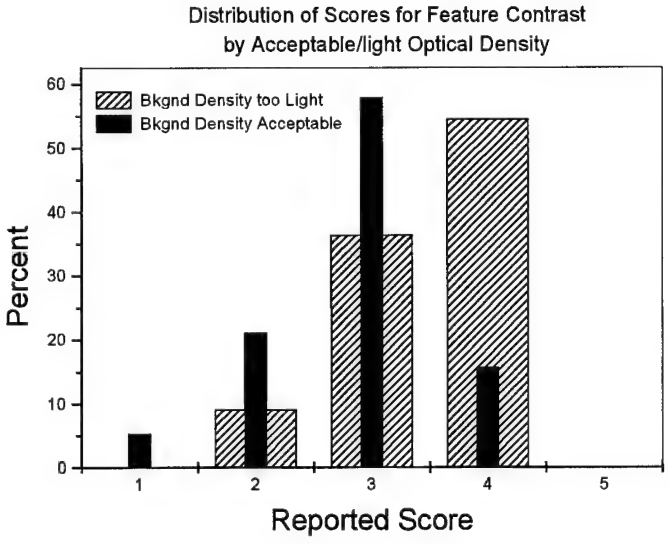

Figure 32. Distributions of reported scores for influence by the prototype on background clutter surrounding features of interest. The scores are distributed for the cases of acceptable film background density and for background density lower than acceptable.

Conclusions

The project has investigated the possibility that commercially available mammography films in use by facilities in the United States have optical polarimetric properties that would allow the manipulation of perceived contrast by the viewer. The method of Azzam was used to perform measurements on the most popular brands of films to determine their Mueller matrix, a mathematical expression of the polarimetric properties of the film. It was found that for all of the films studied, there existed essentially no relationship of any observed polarimetric behavior with optical density under the conditions investigated. Further it was discovered that the source of those polarimetric properties observed is most likely the base of the film, and not due to the presence of developed film emulsion. Two independent series of experiments were conducted to establish the validity of this conclusion.

Extensive research on the spectral response of the films was not conducted on the films tested since the ultimate goal of the project was to develop a device that would compliment the use of standard viewboxes. These devices use fluorescent tubes and produce a light of broad spectral character. It was felt that radiologists would strongly resist viewing a mammogram with a relatively monochromatic light source (i.e. green light, or blue light).

Despite the findings of the polarimetry experiments, it was decided to develop a simple device that would influence the polarimetric state of light transmitted by mammography films viewed on a lightbox. Two radiologists were asked to view a series of mammograms containing various structural features. A subset of the films possessed differing levels of background optical density in order to observe the response by the readers to this parameter. The readers found that for most of the cases, there was little influence by the prototype device on the perceived level of mammography image quality. The results did show that there was some level of improvement observed by the reader for those films having a lower optical background density than acceptable by the respective reader. This may be due in part, however, to the improved response by the human eye to the levels of light resulting from the introduction of the polarizers, which tend to reduce the transmission by the film noticeably. The human eye has a characteristic response to light which is not unlike that of radiographic films. Hence reducing the background level of ambient light received by the eye can allow it to function in more receptive region of response.

Suggestions for Further Research

The project has attempted to improve the level of image quality of film-screen mammograms, a modality of mammography that has been firmly established by the radiological community. Digital methods will become more available as well as powerful in their ability to manipulate the data so collected. However it will be some time before the ability of digital modalities to record *and* render visible the information necessary for quality mammography exceeds that of film-screen technology. This will especially hold with regard to spatial detail, where currently available digital systems just now appearing on the market still lag behind film-screen technology by a significant amount, in our opinion. The authors thus urge continued support of research that will yield improved diagnostic value to screen-film mammography.

The authors are very grateful to the Department of Defense for funding this research. We will recognize the Department of Defense for its support in any and all work related to this project that is published or presented. We would like to thank William Sacks, M.D. and Charles Finder, M.D. for evaluating the prototype viewing device. We also wish to thank Steve Jones and Jane Tuttle-Kuhm for their support in many aspects of the project. Finally, we are also grateful to Orhan Suleiman, Ph.D. and to the management of the Division of Mammography and Radiation Programs.

References

[1] Martin J. Tovée. An Introduction to the Visual System. Cambridge University Press, Cambridge CB2 1RP. 1996.

[2] R.M.A. Azzam. Photopolarimetric measurement of the Mueller matrix by Fourier analysis of a single detected signal. Optics Letters. 2(6), June 1978.

[3] Goldstein DH, Chipman RA. Error analysis of a Mueller matrix polarimeter. J. Opt. Soc. Am. A, 7(4), April 1990.

Bibliography

1. David Spelic, Ph.D., Michael S. West, Ph.D., Orhan Suleiman, Ph.D. *Polarimetric Properties of Mammography X-Ray Film*. Poster Presentation at the 1997 U.S. Food and Drug Administration Forum on Regulatory Sciences.